A&A 368, 689–699 (2001)
DOI: 10.1051/0004-6361:20000578

Astronomy & Astrophysics

A fluorescence model of the C_3 radical in comets⋆

P. Rousselot[1], C. Arpigny[2], H. Rauer[3], A. L. Cochran[4], R. Gredel[5], W. D. Cochran[4], J. Manfroid[2], and A. Fitzsimmons[6]

[1] Observatoire de Besançon, BP 1615, 25010 Besançon Cedex, France
[2] Université de Liège, Institut d'Astrophysique, 4000 Liège, Belgium
[3] Inst. for Space Sensor Techn. and Planetary Expl., Rutherfordstrasse 2, Berlin, Germany
[4] Univ. of Texas, Astronomy Dept., Austin, TX 78712-1083, USA
[5] Max-Planck Institut für Astronomie, Königstuhl 17, 69117 Heidelberg, Germany
[6] Queen's University, Physics Dept. BT7 1NN, Belfast, UK

Received 4 December 2000 / Accepted 22 December 2000

Abstract. Theoretical resonance fluorescence calculations are presented of the triatomic C_3 radical and are compared with observations of the C_3 emission in comets Hale-Bopp and de Vico. A theoretical model of the C_3 vibration-rotational structure in the $A^1\Pi_u - X^1\Sigma_g^+$ electronic system is introduced. The model takes into account the detailed structure of the bending mode ν_2 which is responsible for the emission of the 4050 Å group. A total of 1959 levels are considered, with 515 levels in the ground state. The main effort is to model high-resolution spectra of the 4050 Å emission in comets C/1995 O1 Hale-Bopp and 122P/1995 S1 de Vico. The agreement between observed and theoretical spectra is good for a value of the dipole moment derivative of $\frac{d\mu}{dr} \approx 2.5$ Debye Å^{-1}. The modeled C_3 emission exhibits a pronounced Swings effect.

Key words. molecular data – comets: general – comets: individual: C/1995 O1 Hale-Bopp – comets: individual: 122 P/1995 S1 de Vico

1. Introduction

The C_3 radical is a prominent species in comets. It is responsible for one of the brightest emission features in the optical spectrum, the so-called "4050 Å (Swings) group". Despite the fact that the C_3 emission is commonly observed in comets, comprehensive resonance fluorescence calculations of the radical are not available. The omission is partly due to the fact that accurate molecular parameters have not been available until recently.

A first attempt to explain the 4050 Å emission in comets was presented by Denis-Gausset & Sauval (1968). The authors modeled the rotational transitions in the (000–000) band of the electronic $A^1\Pi_u$–$X^1\Sigma_g^+$ system of C_3 bathed in the solar radiation field. By using different methods of calculations they concluded that the observed rotational temperature on the two comets observed (comets Burnham 1959k; Ikeya 1963a) was low (between 50 to 200 K). They computed that such a temperature would imply a significant probability of rotational deexcitation inside the ground vibronic levels, which does not exist, because of the homonuclear nature of C_3.

The explanation of the low rotational C_3 excitation temperature presents a challenge to any effort to model cometary C_3. The C_3 radical has no permanent dipole moment, and a high rotational excitation temperature might be expected, as is the case for the cometary diatomic carbon molecule C_2 (e.g. Arpigny 1976; Gredel et al. 1989). The disagreement of the models of Denis-Gausset & Sauval (1968) with the observations is due to the omission of radiative transitions in vibrational bands not included in their models. The need for a complete fluorescence excitation model, which considers all vibrational bands which contribute to the 4050 Å emission, is thus obvious.

After publication of the pioneering work of Denis-Gausset & Sauval (1968), a number of theoretical calculations and laboratory experiments of the C_3 radical have appeared (Römelt et al. 1978; Becker et al. 1979; Cooper & Jones 1979; Jungen & Merer 1980; Chabalowski et al. 1986; Schmuttenmaer et al. 1990; Baker et al. 1997). These works have given more information concerning the

Send offprint requests to: P. Rousselot,
e-mail: philippe@obs-besancon.fr

⋆ Based on observations made with William Herschel Telescope operated on the island of La Palma by the Isaac Newton Group in the Spanish Observatorio del Roque de los Muchachos of the Instituto de Astrofisica de Canarias, and on observations made at the McDonald Observatory, which is operated by the University of Texas at Austin, USA.

electronic oscillator strength, the Franck-Condon factors and the wavelengths of some poorly known transitions. These new results constrain the molecular parameters of C_3 sufficiently well to allow a comprehensive theoretical modeling of its spectrum. In addition, a number of high-resolution spectra of the 4050 Å group have become available, which are needed to compare the calculations with the observations.

The rotation-vibrational structure of the C_3 radical which is assumed in our calculations is discussed in Sect. 2. Details of the model and the molecular parameters adopted are given in Sect. 3. Section 4 presents our observations of comets Hale Bopp and de Vico, and Sect. 5 contains the comparison of our model spectra with the observed 4050 Å group. The main conclusions are summarised in Sect. 6.

2. The C_3 radical

The study of the C_3 radical is closely related to the study of comets. As a matter of fact, its main emission, which is known as the "4050 Å group" or "Swings group", was first discovered in 1881 by Huggins in one of the first spectroscopic studies of a comet. The 4050 Å emission was studied in great detail by Swings et al. (1941). Since that work, various authors published cometary C_3 spectra of high quality (Dossin et al. 1961; Ferhenbach 1963; Stawikowski & Greestein 1964).

The pioneering work was published by Gausset et al. (1965). That paper was based on the laboratory data available then. It included a detailed analysis of the vibrational structure of the ν_2 bending mode from which the 4050 Å emission arises. The study gave the wavenumbers of the different rotational lines of the 4050 Å group, an identification of the different vibrational levels which are involved, and the basic vibrational and rotational constants of the vibrational states. As one of the main results, Gausset et al. (1965) concluded that the bending frequency ν_2 is very small, with a value of about 63 cm^{-1} in the $X^1\Sigma_g^+$ electronic ground state. The small value implies that a multitude of vibrational levels are significantly populated, even at low temperatures. This creates a complex vibrational structure in the laboratory absorption spectra.

Figure 1 represents the vibrational structure of the C_3 radical. The figure shows in detail the various vibrational states which correspond to the different values of the bending mode v_2. The 4050 Å group arises from transitions in the $A^1\Pi_u \rightarrow X^1\Sigma_g^+$ system. Figure 1 discriminates the various vibrational levels in the upper and lower electronic states. In both states the three vibrational quantum numbers v_1, v_2 and v_3 are given. v_1 is the symmetric and v_3 is the anti-symmetric stretching mode.

In the $X^1\Sigma_g^+$ electronic ground state, the l value is added to v_2. The quantum number l is the total vibrational angular momentum: $l = \mid \sum_i(\pm l_i) \mid$. Since $v_1 = v_3 = 0$, allowed values of l are v_2, $v_2 - 2$, etc. Lowest angular momentums are 0 or 1, depending if v_2 is even or odd. The total vibrational angular momentum is given by the sum of the electronic orbital angular momentum Λ and l. For the electronic ground state, $\Lambda = 0$, and the angular momentum of the vibrational state is directly given by l. We obtain Σ states for $l = 0$, Π states for $l = 1$, Δ state for $l = 2$, and so forth.

In the $A^1\Pi_u$ electronic state, where $\Lambda = 1$, the vibronic angular momentum is given by the quantum number K, which is defined by $K = \mid \pm \Lambda \pm l \mid$. In Fig. 1 the vibrational state defined by K as well as the v_1, v_2 and v_3 values are explicitly given.

Examination of the energy level diagram shows that two different types of electronic transitions exist. Firstly, transitions between two vibrational states of even v_2 value are allowed. Secondly, there are transitions which involve odd values of v_2. The existence of these two distinct types of transitions is a consequence of the quantum mechanical selection rules. For the linear-linear transitions (i.e. when the structure of the molecule appears linear, or quasi-linear, in both the lower and upper states) allowed electronic transitions combine two states with the same value of l (Herzberg 1966). Table 1 summarises all the transitions which obey this selection rule.

Table 1. Possible vibronic transitions, according to the selection rule mentioned in the text

v_2'	K	vibrational state (upper state)	Ground vibrational state with which a transition is possible
	0	Σ_g^+	Π_u
	2	$\Delta_g^{(+)}$	Π_u or Φ_u
	4	$\Gamma_g^{(+)}$	Φ_u or H_u
5	6	I	H_u
	4	$\Gamma_g^{(-)}$	Φ_u or H_u
	2	$\Delta_g^{(-)}$	Π_u or Φ_u
	0	Σ_g^-	Π_u
	1	$\Pi_u^{(+)}$	Σ_g^+ or Δ_g
	3	$\Phi_u^{(+)}$	Δ_g or Γ_g
4	5	H_u	Γ_g
	3	$\Phi_u^{(-)}$	Δ_g or Γ_g
	1	$\Pi_u^{(-)}$	Σ_g^+ or Δ_g
	0	Σ_g^+	Π_u
	2	$\Delta_g^{(+)}$	Π_u or Φ_u
3	4	Γ_g	Φ_u
	2	$\Delta_g^{(-)}$	Π_u or Φ_u
	0	Σ_g^-	Π_u
	1	$\Pi_u^{(+)}$	Σ_g^+ or Δ_g
2	3	Φ_u	Δ_g
	1	$\Pi_u^{(-)}$	Σ_g^+ or Δ_g
	0	Σ_g^+	Π_u
1	2	Δ_g	Π_u
	0	Σ_g^-	Π_u
0	1	Π_u	Σ_g^+

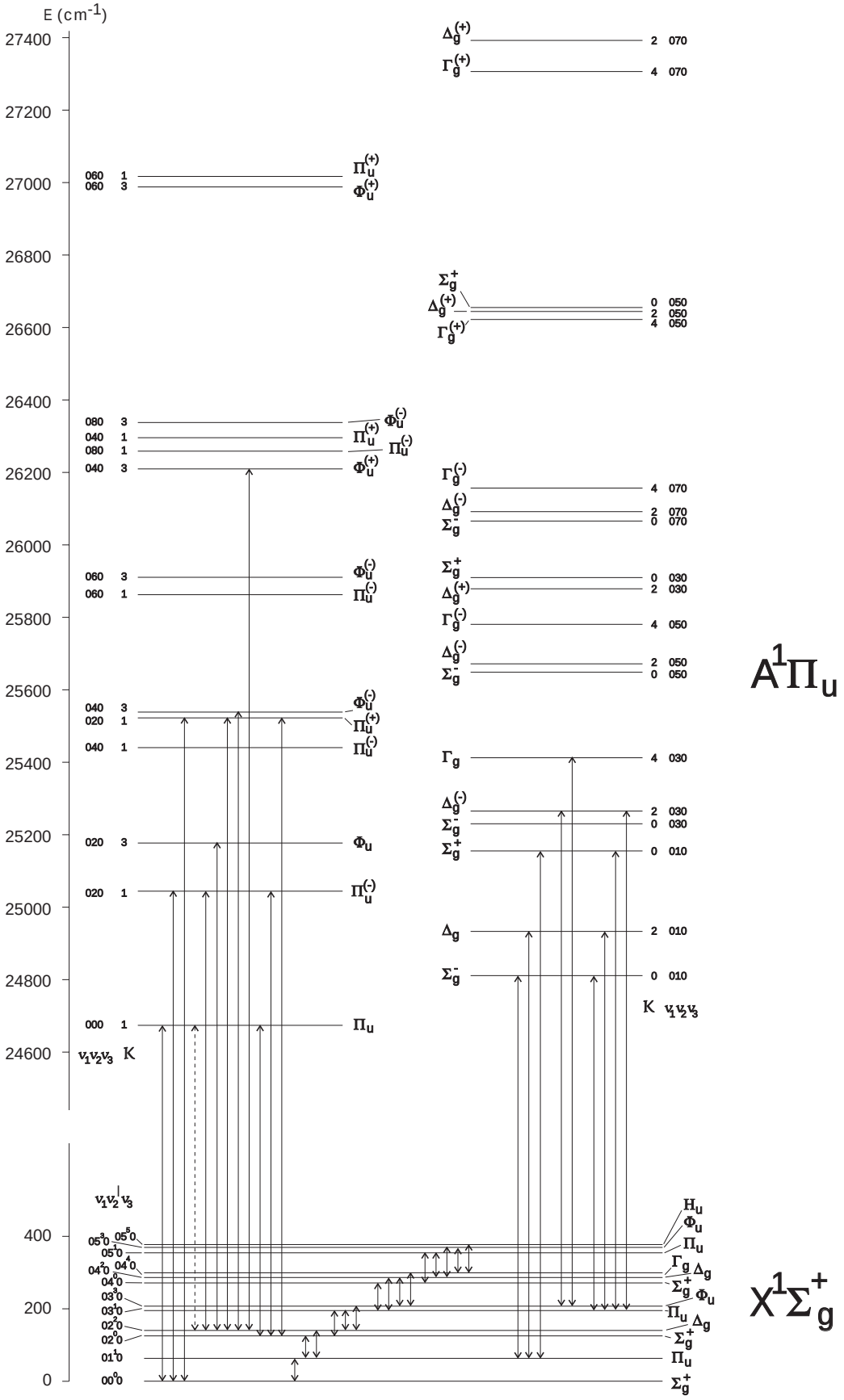

Fig. 1. Energy level diagram of the C_3 radical (see the text for more details)

An exception to this rule was mentioned by Gausset et al. (1965). There are a number of $\Pi_u \rightarrow \Delta_g$ transitions within the (000−020) vibrational bands. They are possible for the even rotational J values of the Δ_g state. Their existence is due to a particularly strong interaction between the vibrational and rotational angular momenta.

Figure 2 contains the rotational structure of the different transitions which occur between the two electronic states. C_3 is a homonuclear molecule and all antisymmetric levels are missing. For completeness, the antisymmetric levels are given by dashed lines in Fig. 2.

Within the electronic ground state, pure vibrational transitions may occur. The pure vibrational transitions establish a link between the two systems of transitions discussed above. It is because of these transitions that the population distribution in the higher vibrational *and* rotational levels of the ground state are depopulated. As a result, the corresponding excitation temperatures are low. The pure vibrational transitions involve $\Delta v_2 = 1$ only. These transitions have been detected in absorption in the interstellar medium (Hinkle et al. 1980).

3. The model

In order to model the C_3 fluorescent spectrum in comets, we have considered a significant number of vibrational and rotational levels. All 45 vibrational levels which appear in Fig. 1 are included in our statistical equilibrium calculations. Each vibrational state contains rotational levels with rotational quantum number J less than or equal to 50. The total number of levels included in the model is 1959, out of which 515 rotational levels are in the $X^1\Sigma_g^+$ ground state.

In the model calculations, we omit a few vibronic states with excitation energies less than 27 400 cm^{-1}. In particular, we neglect levels in (100), (040), (050), (060), and (070) which are characterised by a high value of K. The influence of these levels in our calculations is probably weak, because they interact only with the ground vibrational states of a high energy level.

The band transition probabilities $A_{v'v''}$ are given by

$$A_{v'v''} = \frac{8\pi^2 e^2}{mc} \tilde{\nu}^{*2}(\mathrm{cm}^{-1}) \frac{g_\mathrm{l}}{g_\mathrm{u}} f_{v'v''} \quad (1)$$

where $\frac{8\pi^2 e^2}{mc} = 0.667$ in cgs unit, $\tilde{\nu}^*(\mathrm{cm}^{-1})$ is the wavenumber corresponding to the band-head, g_l and g_u are the lower and upper statistical weight, respectively, and $f_{v'v''}$ is the band absorption oscillator strength. The ratio of the statistical weights is $g_\mathrm{l}/g_\mathrm{u} = 1/2$.

We adopt $f_{v'v''} = f_\mathrm{el} \times \frac{\tilde{\nu}^*(\mathrm{cm}^{-1})}{\nu_{000}} \times q_{v'v''}$, where f_el is the electronic oscillator strength (absorption) for the $A^1\Pi_u - X^1\Sigma_g^+$ transition, $q_{v'v''}$ is the Franck-Condon factor, and $\nu_{000} = 24\,685$ cm^{-1} is the frequency of the (000–000) band.

A value of $f_\mathrm{el} = 0.035$ is adopted for the electronic oscillator strength (Weltner & Van Zee 1989). There exists a discrepancy between the theoretical calculations of f_el and laboratory measurements. While most of the theoretical calculations have now converged to $f_\mathrm{el} \simeq 0.05$ (Römelt et al. 1978; Chabalowski et al. 1986), experimental studies report a range of $f_\mathrm{el} \simeq 0.025$ (Becker et al. 1979) to $f_\mathrm{el} \simeq 0.033$ (Cooper & Jones 1979). The value of f_el adopted in our model is intermediate between the theoretical and laboratory results.

The Franck-Condon factors $q_{v'v''}$ have been computed using the overlap integrals calculated by Jungen & Merer (1980). From the band transition probabilities determined above, we infer the line transition probabilities using

$$A_{v'J'v''J''} = \frac{2-\delta_{0,K'}}{2-\delta_{0,K'+K''}} \left(\frac{\tilde{\nu}^3(\mathrm{cm}^{-1})}{\tilde{\nu}^{*3}(\mathrm{cm}^{-1})}\right) \frac{S_{J'J''}}{2J'+1} A_{v'v''} \quad (2)$$

where $\tilde{\nu}(\mathrm{cm}^{-1})$ is the wavenumber of the transition and $\tilde{\nu}^*(\mathrm{cm}^{-1})$ the wavenumber of the band-head. The value J' is the rotational quantum number of the upper state, and $S_{J'J''}$ is the Hönl-London factor. This formula is similar to expressions used for diatomic molecules, with the electronic angular momentum Λ replaced by the vibronic angular momentum K. The similarity to the diatomic molecule case results from the quasi-linear structure of C_3 (Weltner & Van Zee 1989; Herzberg 1966).

The Hönl-London factors are obtained from the formulae given by Herzberg (1950) for the symmetric top (again replacing the Λ values by the K values). The following sum rule has been used for these factors:

$$\sum_{p',p''} \sum_{\Sigma',\Sigma''} \sum_{J''} S_J = (2-\delta_{0,K'+K''})(2S+1)(2J+1). \quad (3)$$

The line transition probabilities $B_{v''J''v'J'}$ for the absorption processes are related to the Einstein $A_{v'J'v''J''}$ coefficients by:

$$B_{v''J''v'J'} = 6.01038\ 10^{24} \frac{1}{\tilde{\nu}^3(\mathrm{cm}^{-1})} \frac{2J'+1}{2J''+1} A_{v'J'v''J''}. \quad (4)$$

Finally, the absorption probabilities are obtained from the B-values after multiplication with the solar radiation density ρ_ν in units of erg cm^{-3} Hz^{-1}. We have used the high-resolution solar spectrum published by Kurucz et al. (1984) from 2960 to 13 500 Å (these data are available online from NSF/NOAO). Above this wavelength, i.e. from 13 500 Å to 1 mm, we have used some data published by Thekaekara (1974), which have a lower resolution. As most of the transition wavelengths are known with good accuracy (i.e. typically a few hundreths of Å or less) it is possible to demonstrate the effects of varying velocities of the comet with respect to the sun.

The excitation energies of the energy levels were computed from the experimental wavelengths given by Gausset et al. (1965). In cases where wavelengths are not available, we used the molecular constants given by the same authors. For the $A^1\Pi_u$ electronic state we include a number of vibrational energy levels calculated by Jungen & Merer (1980). For the excited vibronic states of the $A^1\Pi_u$ electronic state, the mean rotational constant B_v for this electronic state given by Herzberg (1966) is used.

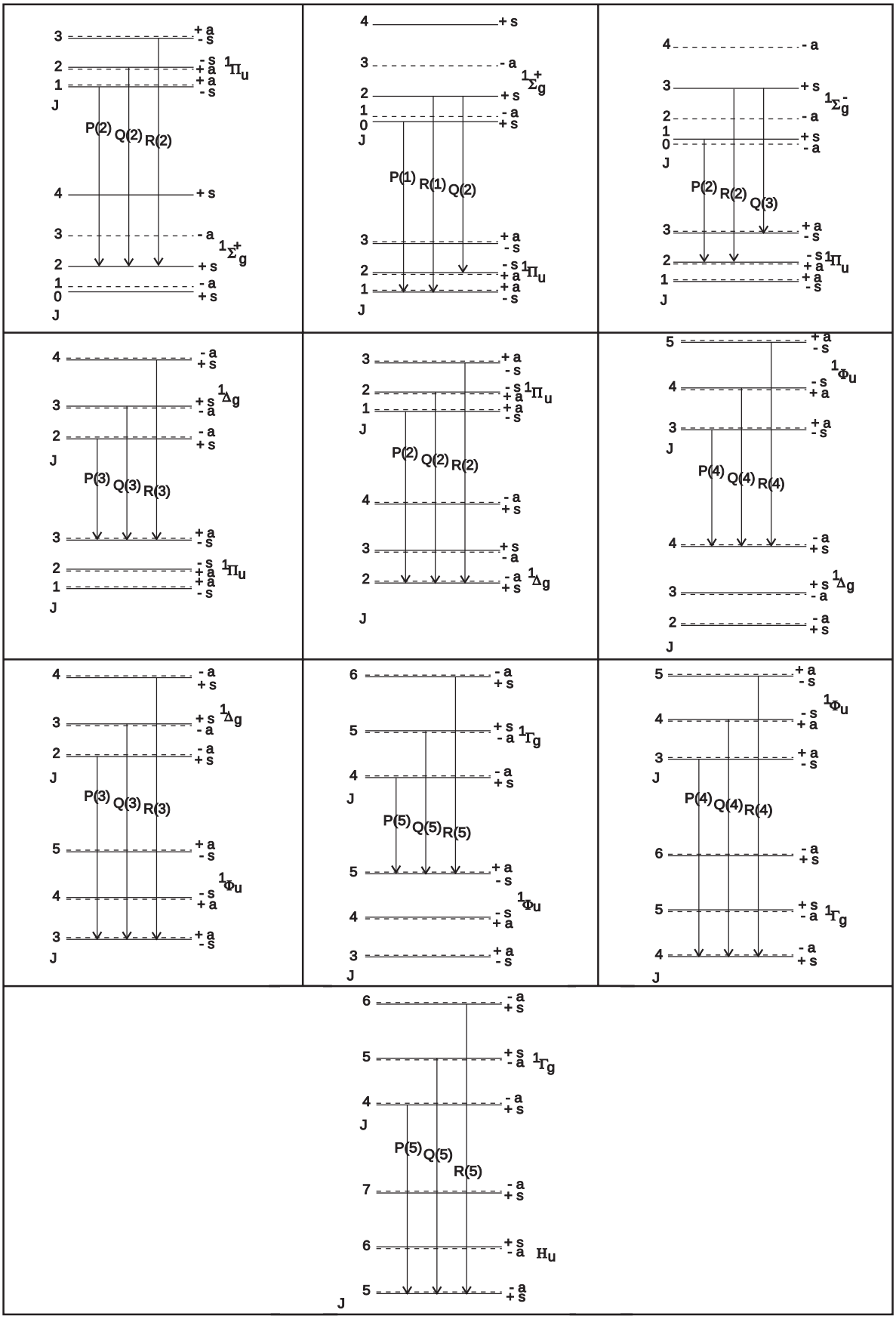

Fig. 2. Details of the rotational structure of the different transitions appearing in Fig. 1

For the (06^-0) and (04^+0) vibronic levels we use the values published by Baker et al. (1997).

To calculate the band transition probabilities of the pure vibrational transitions with $\Delta v_2 = 1$, we use the harmonic oscillator relation as given by Clegg & Lambert (1982),

$$A(v_2 + 1 \rightarrow v_2) = 5.3\ 10^{-6}(v_2 + 1)\frac{\omega_e^2}{\bar{\mu}}\left(\frac{\mathrm{d}\mu}{\mathrm{d}r}\right)^2\ \mathrm{s}^{-1} \qquad (5)$$

where ω_e is the vibrational frequency in cm^{-1}, $\bar{\mu}$ is the reduced mass expressed in amu and $\frac{\mathrm{d}\mu}{\mathrm{d}r}$ is the dipole moment derivative in units of Debye $\mathrm{Å}^{-1}$. The reduced mass for C_3 is $\bar{\mu} = 4$. Clegg & Lambert (1982) used the results of the computation of the charge transfer published by Clementi & Clementi (1962) to estimate the dipole moment derivative. In C_3, the central C atom carries a positive charge of 0.79e. The calculations by Clementi & Clementi (1962) suggest a value of $\frac{\mathrm{d}\mu}{\mathrm{d}r} \simeq$ 3.8 Debye $\mathrm{Å}^{-1}$ for the dipole moment derivative, but the authors considered their results as "provisional". It turns out that the strength of the pure vibrational transitions is a crucial point in our model. Because its value is not accurately constrained from the theoretical calculations, we treat the dipole moment derivative as a free parameter in our calculations.

The corresponding rotation-vibrational line transition probabilities are computed using Hönl-London factors for the symmetric top molecules. This treatment is similar to treatment of the electronic transitions discussed above.

The computed line transition probabilities for spontaneous emission and absorption are collected in a matrix P, with matrix elements P_{ij} being the transition probability from level i to level j, $A_{v'J'v''J''}$ for indices $i > j$, and $B_{v''J''v'J'}\rho_\nu$ for indices $i < j$. The dimension of the matrix P is given by the total number of energy levels considered here. The P-matrix is treated in the formalism of the matrix method of Zucconi & Festou (1985). Their code is used to compute the equilibrium solution by solving a linear set of algebraic equations. The dimension of the linear set of equations is determined by the number of ground energy levels minus 1, or 514 independent equations in our case.

The calculated relative level populations of the ground states are subsequently being used to compute the population distribution among the excited vibration-rotational levels. Explicitly, the relative population x_i of level i in the $A^1\Pi_u$ state is obtained from:

$$\sum_{j=1}^{N_X} B_{ji}\rho_\nu x_j \simeq \sum_{j=1}^{N_X} A_{ij}x_i \qquad (6)$$

$$x_i \simeq \frac{\sum_{j=1}^{N_X} B_{ji}\rho_\nu x_j}{\sum_{j=1}^{N_X} A_{ij}}. \qquad (7)$$

The synthetic spectrum is obtained finally from the equilibrium population distribution and the transition probabilities $A_{v'J'v''J''}$ by convolution with Gaussians.

4. Observations of comets Hale-Bopp and de Vico

The observations used to test our model were obtained on comets C/1995 O1 Hale-Bopp and 122P/1995 S1 de Vico. Comet Hale-Bopp was observed on April 18, 1997 at 21 h 16 mn UT. The spectrum was obtained with the 4.2 m William Herschel telescope at the La Palma observatory in Spain using the Utrecht Echelle Spectrograph (UES). The spectral resolution of UES is 0.04 Å/pixel or 0.1 Å. The aperture of the spectrometer was centered at 10 arcsec from the nucleus position, defined as the maximum in the brightness distribution. This allows enhancement of the contrast of gas emission to the continuum level. The exposure time was 260 s. Each order was bias and scattered light subtracted, and flat-fielded. The blaze profile was calculated for each spectral order from the flat field exposures, and divided out. We have focused our study on the (000–000) band, around 4052 Å. The underlying solar continuum was estimated from an integration on the moon, and was subtracted by adjusting the continuum level at the blue and red end of the spectrum where no molecular emission is present.

At the time of the observation, the heliocentric velocity of the comet was 10.0 km s^{-1}, its heliocentric distance 0.97 AU and its geocentric velocity 27.4 km s^{-1}. The wavelength calibration was computed in the laboratory rest-frame and air wavelengths. The spectrum of comet Hale-Bopp is shown in Fig. 3. The C_3 emission near 4050 Å is clearly detected, and the rotational structure away from the band-head is resolved.

The spectrum of comet deVico was obtained on October 4, 1995 starting at 11 h 10 mn UT with the 2DCoudé spectrograph on the 2.7-m telescope at McDonald Observatory (USA, TX). The 2DCoudé instrument is a cross-dispersed echelle spectrograph located at the f/33 coudé focus of the telescope. The exposure time was 1500 s. Data reduction has been described by Cochran et al. (2000). The spectral resolution in order 85, the order with the C_3 (000–000) band, was measured using observations of a thorium arc lamp as 0.073±0.003 Å (two pixels). The comet was observed with a slit of width 1.2 arcsec and a length of 8.2 arcsec with the cometary optocenter offset slightly towards one end of the slit. The solar spectrum was observed with the same instrumental setup by imaging solar light through a diffusing port on the roof of the coudé slit room. The solar spectrum was shifted onto the cometary frame and the solar spectrum was removed with appropriate weighting to remove the continuum. Then the resultant spectrum was shifted to the laboratory rest frame. The heliocentric distance of the comet was 0.66 AU and its heliocentric velocity −1.7 km s^{-1}. The spectrum of comet de Vico is shown in Fig. 4. Again, the 4050 Å emission is detected, and the rotational structure is resolved.

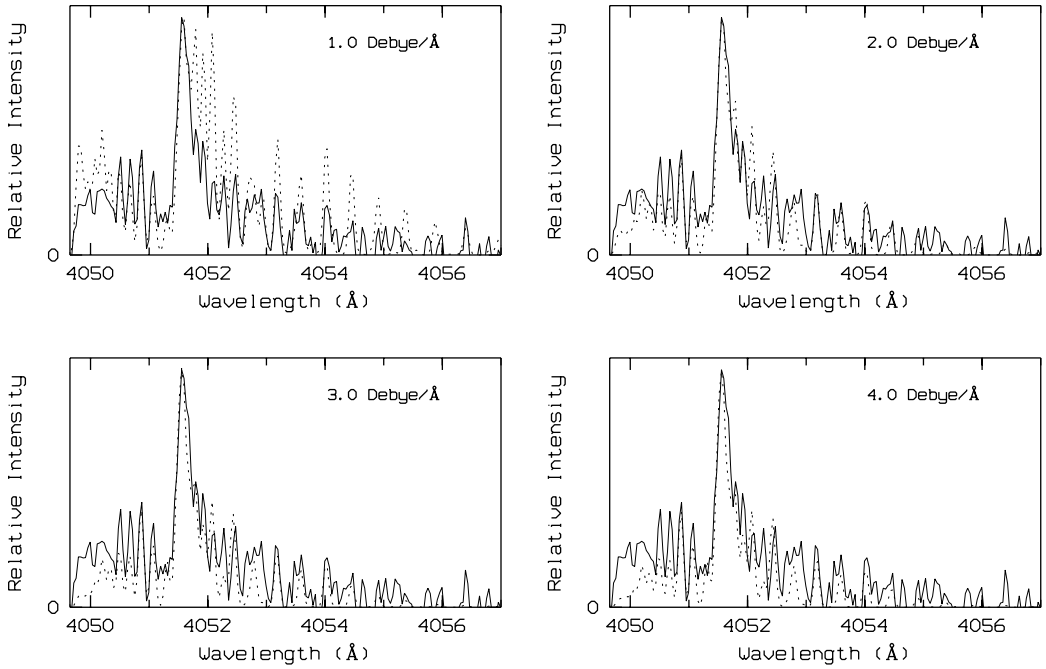

Fig. 3. Observed spectrum of comet Hale-Bopp (bold line) and synthetic spectra obtained (dashed lines) for values of the dipole moment derivative of 1, 2, 3, and 4 Debye $Å^{-1}$

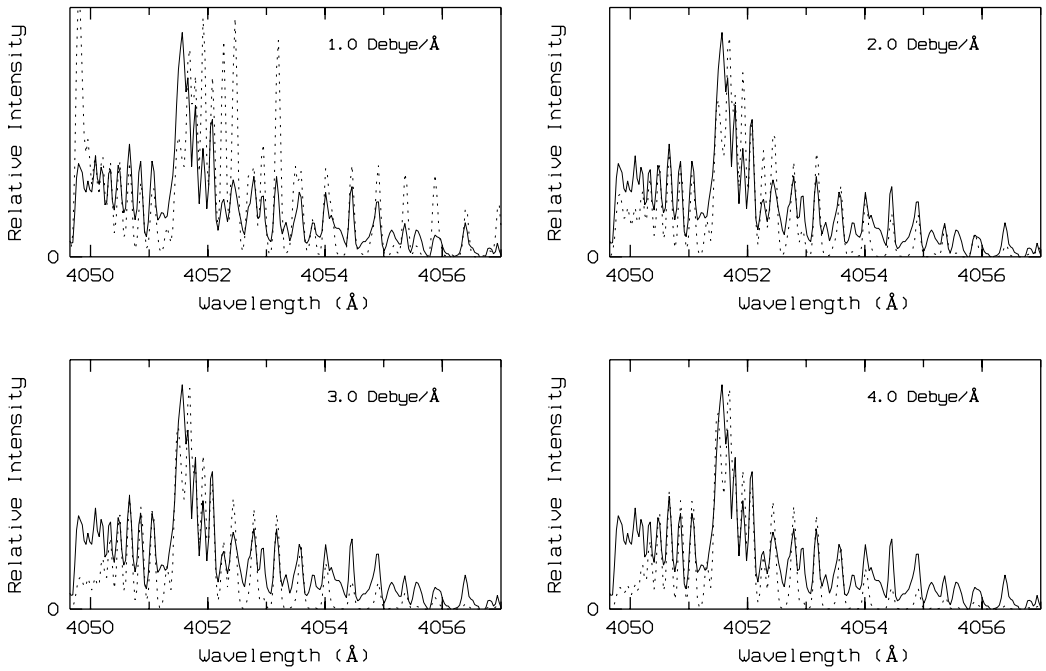

Fig. 4. Observed spectrum of comet de Vico (bold line) and synthetic spectra (dashed lines) obtained for values of the dipole moment derivative of 1, 2, 3, and 4 Debye $Å^{-1}$

5. Results

Apart from the dipole moment derivative which is used as a free parameter in our model, some of the molecular parameters used here may require some adjustment. This is true in particular for the value of the electronic oscillator strength and for the Franck-Condon factors. Note however that changes in the electronic oscillator strength may be compensated for by changes in the dipole moment derivative. This is because the rotational excitation temperature is governed by two competing processes, firstly by the electronic transitions and secondly by the pure vibrational transitions. Variations in the electronic oscillator strength may thus be controlled by changes in the dipole moment derivative.

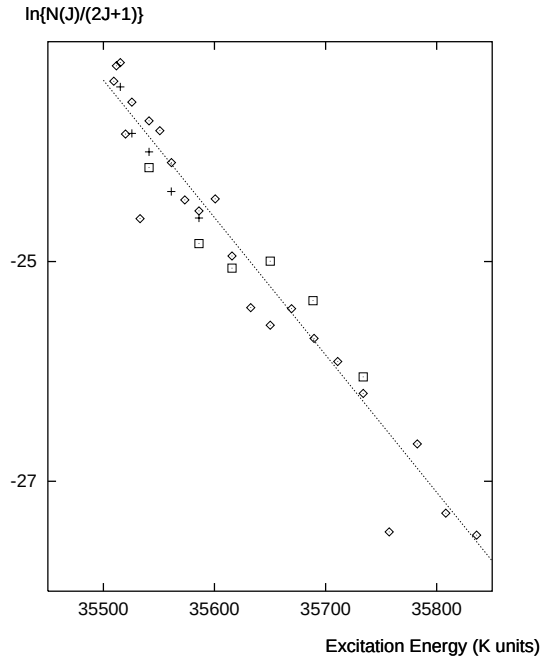

Fig. 5. Excitation diagram of rotational levels in the $A^1\Pi_u$ 000 vibrational state. Data inferred from the R-branch and P-branch transitions (see text) are given by crosses and squares, respectively. Diamonds are obtained from the synthetic spectrum calculated for comet de Vico for the date of the observations, and a dipole moment derivative of 2.5 Debye Å^{-1}. The dashed line corresponds to a rotational excitation temperature of 80 K

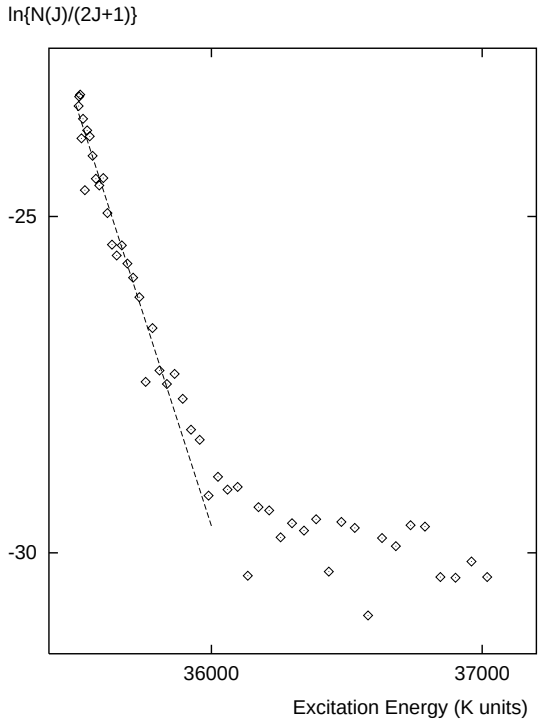

Fig. 6. Excitation diagram constructed for rotational levels in the $A^1\Pi_u$ 000 vibrational state, obtained from the synthetic spectrum of comet de Vico and a dipole moment derivative of 2.5 Debye Å^{-1} (see text). The straight line is a fit to the population distribution in rotational levels with $J \leq 28$. The corresponding rotational excitation temperature is 80 ± 10 K

In a first analysis, we constrain the dipole moment derivative in order to fit the high-resolution spectrum obtained on comet Hale-Bopp. The synthetic spectra obtained from the model are highly sensitive to the dipole moment derivative. The best fit is obtained for a value of $2 \leq \frac{\mathrm{d}\mu}{\mathrm{d}r} \leq 3$ Debye Å^{-1}. This is shown in Figs. 3a-d which contain a comparison of the observed spectrum of comet Hale-Bopp with synthetic spectra obtained for values of $\frac{\mathrm{d}\mu}{\mathrm{d}r} = 1$, 2, 3, and 4 Debye Å^{-1}, respectively.

A similar analysis was performed using the spectrum of comet de Vico. For this spectrum we have used a spectral resolution for the synthetic spectrum slightly greater to the one computed from the calibration lamp (i.e. 0.09 Å instead of 0.073 Å). The reason is that a detailed analysis of the unblended C_3 emission lines lead to this value. The broadening of these lines can be explained in terms of a small Doppler broadening inside the coma. The results are shown in Figs. 4a-d, again for values of $\frac{\mathrm{d}\mu}{\mathrm{d}r} = 1$, 2, 3, and 4 Debye Å^{-1}, respectively. As for comet Hale-Bopp, the best fit to the observed spectrum is obtained for a value of $2 \leq \frac{\mathrm{d}\mu}{\mathrm{d}r} \leq 3$ Debye Å^{-1}.

A close inspection of Figs. 3 and 4 show some deviations between the theoretical and the observed spectra in both comets. We feel that uncertainties in the subtraction of the solar continuum cause some of the discrepancies observed. Note also that the Hönl-London factors used in the model are approximate. The latter may explain a too rapid decrease in the intensity of the emission from the higher J values which is apparent in both Figs. 3 and 4.

We have calculated rotational excitation temperatures from our synthetic population distributions. In order to compare the results inferred for comet de Vico with the model results, we have plotted the intensities of some unblended lines in an excitation diagram with values of $\ln\{N(J)/(2J+1)\}$ plotted versus the excitation energy of the corresponding rotational level J. $N(J)$ is the relative population density in J. The observed intensity I is transformed to $N(J)/(2J+1)$ by use of $(I/\tilde{\nu}^3(\mathrm{cm}^{-1}))(1/S_{J'J''})$. In our spectrum we measure the intensity for five R-branch lines (R(2), R(4)... R(10)) and for six P-branch lines (P(8), P(12), P(14)... P(20)). The results are shown in Fig. 5, with data points inferred from the R-branch and P-branch transitions represented by crosses and squares, respectively. Also included in the excitation diagram of Fig. 5 are the model results obtained from a dipole moment derivative of 2.5 Debye Å^{-1} (diamonds). The dashed line corresponds to a rotational excitation temperature of 80 K.

Figure 6 represents the excitation diagram obtained from the synthetic population distribution of all rotational levels in the electronic ground state, again obtained from the model set up for comet de Vico and a dipole moment derivative of $\frac{\mathrm{d}\mu}{\mathrm{d}r} = 2.5$ Debye Å^{-1}. The rotational levels ($J \leq 28$) follow a Boltzmann distribution and are characterised by an excitation temperature of $T_{\mathrm{rot}} = 80 \pm 10$ K.

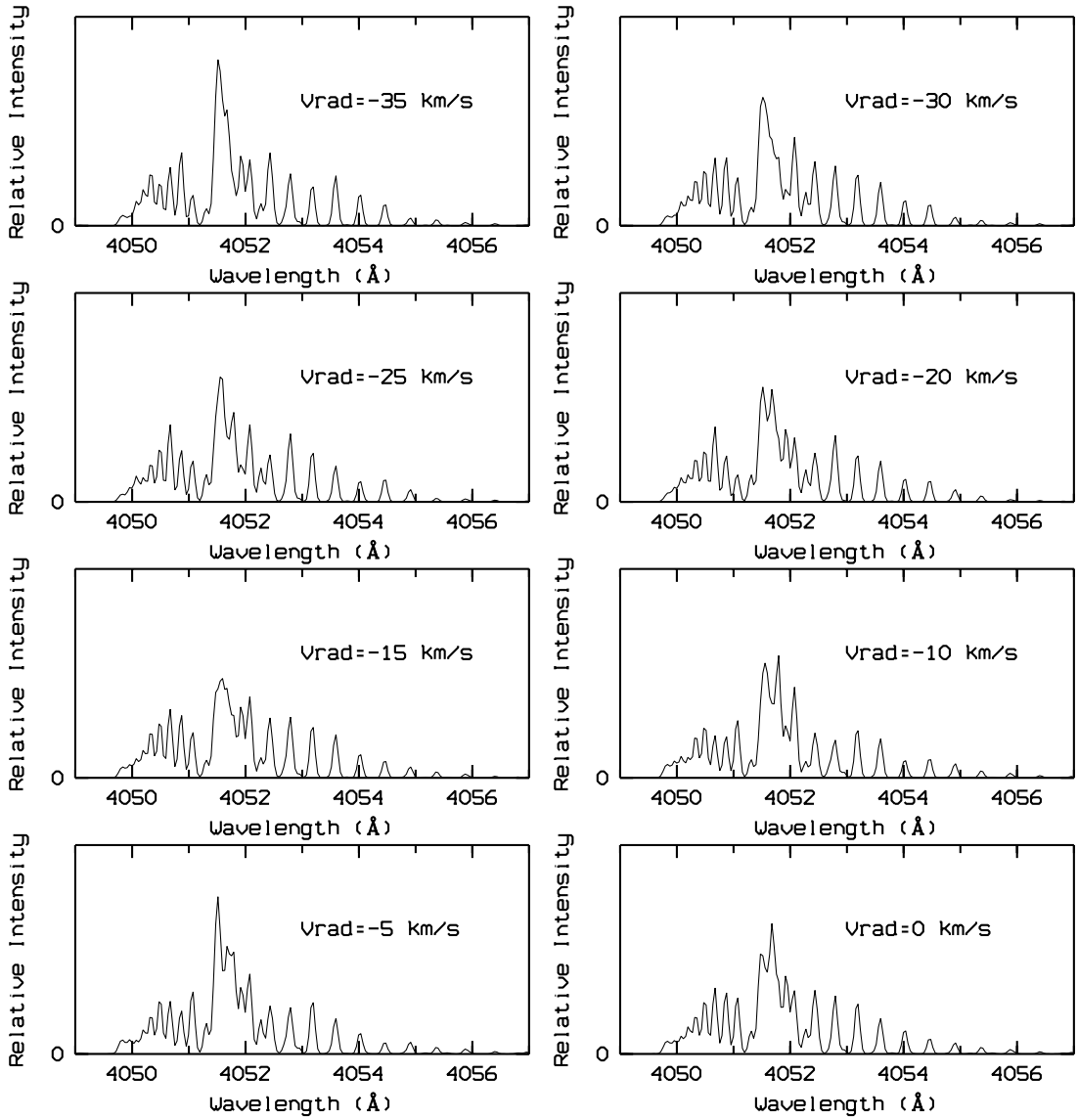

Fig. 7. Synthetic spectra of the $000 - 000$ ($\Pi_u - \Sigma_g^+$) band of the C_3 spectrum obtained at 1 AU of heliocentric distance and for different values of the heliocentric velocity. All the intensities are plotted on a common scale

This temperature is consistent with the range of 50–200 K estimated by Denis-Gausset & Sauval (1968) based on some experimental spectra obtained on comets Burnham (1959k) and Ikeya (1963a).

It is one of the main conclusions of the present paper that the rovibrational transitions in the electronic ground state explain the low rotational excitation temperature of the 4050 Å group in comets. A test was performed by using a very weak value of the dipole moment derivative ($\frac{\mathrm{d}\mu}{\mathrm{d}r} = 10^{-4}$ Debye Å^{-1}) and a heliocentric distance of 1 AU. The rotational excitation temperature was found to be about 800 K. This result shows it is impossible to model correctly the C_3 spectrum without using a realistic rovibrational decay in the ground electronic state.

Our model calculations show that the Swings effect is important in the resonance fluorescence excitation of cometary C_3. The Swings effect, or the dependence of the C_3 emission on the heliocentric velocity of the comet, is shown in synthetic spectra of the 4050 Å group for a large range of heliocentric radial velocities (Figs. 7 and 8). In all calculations, the heliocentric distance is 1 AU and the dipole moment derivative is 2.5 Debye Å^{-1}. The spectra are convolved with an instrument response function with 0.1 Å full width at half maximum (FWHM). The Swings effect influences strongly the observed spectra. It is clear that the high spectral resolution in the solar radiation field is required in the modeling of cometary C_3.

We have also investigated the effect of the heliocentric distance upon the C_3 emission. Figure 9 shows the synthetic spectra obtained for heliocentric distances of 0.5, 1.5, 2.0, 2.5, 3.0 and 3.5 AU. In all calculations, the heliocentric velocity is +10 km s^{-1} and the dipole moment derivative is 2.5 Debye Å^{-1}. With increasing heliocentric distance, the rotational temperature decreases significantly.

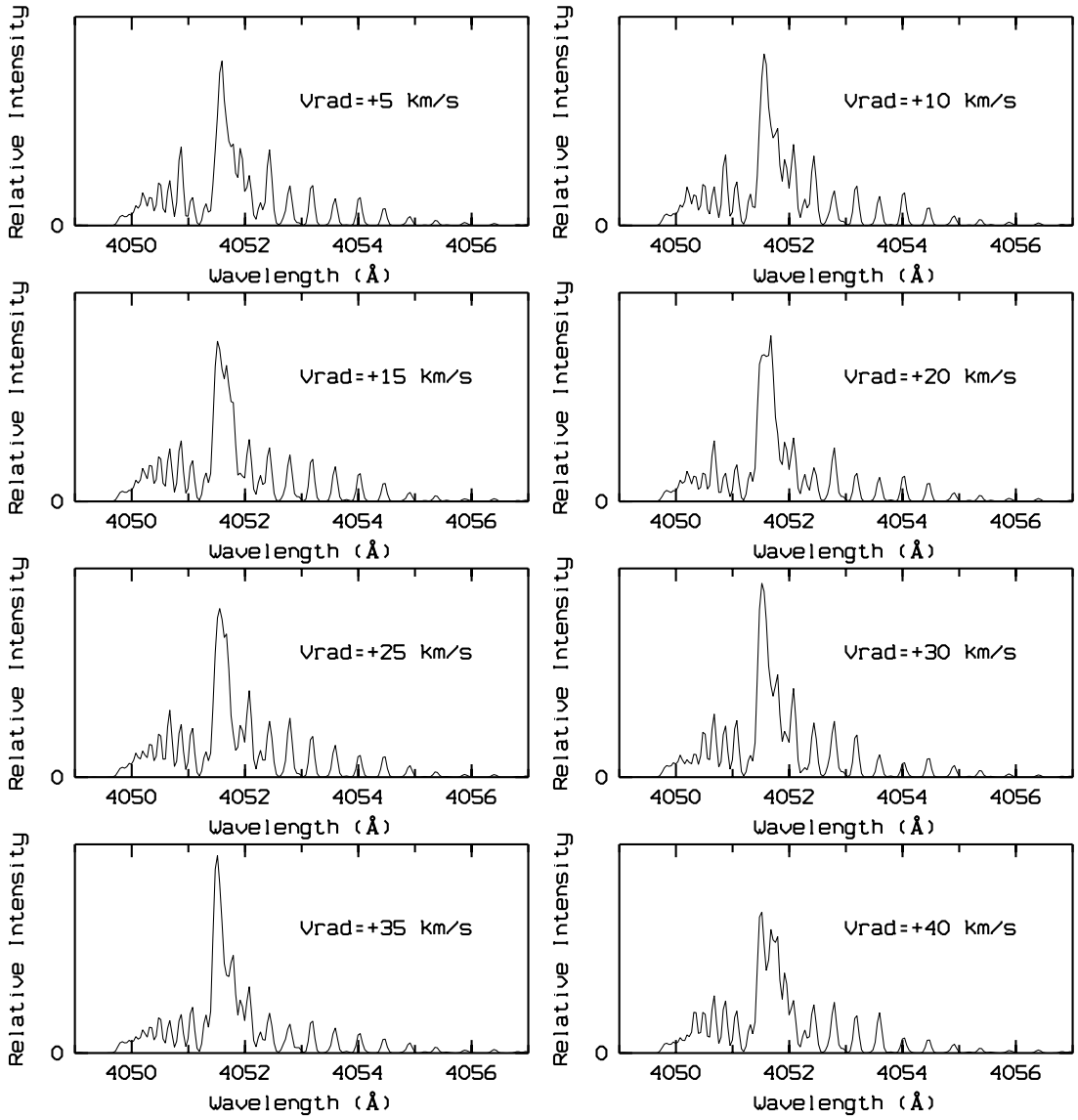

Fig. 8. See Fig. 7, continued

6. Summary

We have presented the first comprehensive statistical equilibrium calculations of the resonance fluorescence mechanism of the C_3 radical in comets. We have shown that the low rotational temperature of the (000–000) band of the C_3 emission in comets is explained by an efficient depopulation of the rotational levels by pure rotation-vibration transitions in the electronic $X^1\Sigma_g^+$ ground state. We have fitted satisfactorily the observed rotational distribution of the 4050 Å group in comets Hale-Bopp and de Vico. The best agreement of the theoretical spectra with the cometary emission is obtained for a value of the dipole moment derivative of 2.5 Debye $Å^{-1}$.

The model does not take into account a number of transitions which may affect the C_3 population distribution. Firstly, vibrational states which correspond to the symmetric and the anti-symmetric stretching modes (i.e. vibrational states with v_1 and v_3 different of zero) are not included. Secondly, by analogy to diatomic molecular carbon, electronic transitions to the $a^3\Pi_u$ and $B^1\Sigma_u^+$ may be important. It is known from the C_2 resonance fluorescence (Gredel et al. 1989) that transitions into the singlet B and triplet a state do affect the population distribution in the singlet X electronic ground state. Note however that rotational constants of the triplet a and singlet B states are not available. Thirdly, the observed high-resolution spectra are obtained close to the nucleus of the comets. The possibility exists that the C_3 population distribution in the inner coma has not reached statistical equilibrium, and that collisional quenching may affect the population distribution. It would be most illustrative to obtain simultaneous C_3 spectra in the inner and outer coma of a comet, say centered on the nucleus and at a large cometocentric distance of more than about 100 000 km. A comparison of both spectra will show whether C_3 has reached statistical equilibrium and whether collisions are important. Because of the fast decrease of the intensity of C_3 from the nucleus,

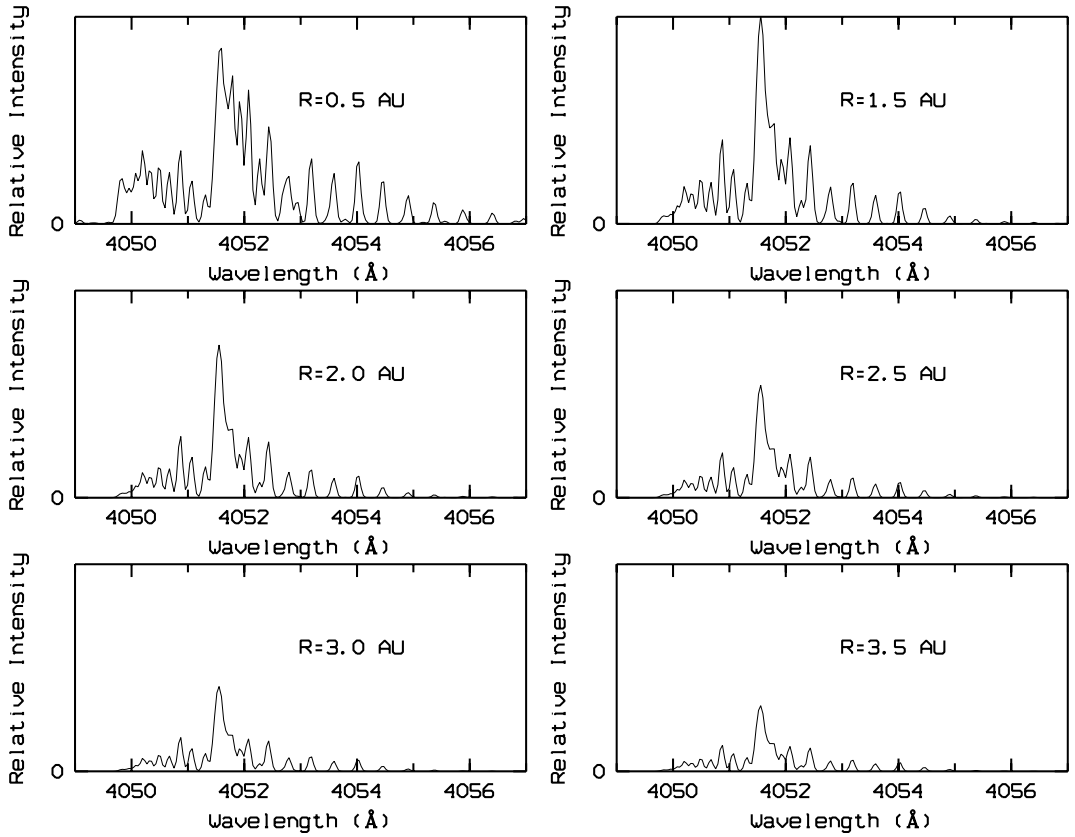

Fig. 9. Synthetic spectra of the 000−000 ($\Pi_u - \Sigma_g^+$) band of the C_3 spectrum obtained for different heliocentric distances. In all calculations, the radial velocity is +10 $\mathrm{km\,s^{-1}}$ and the dipole moment derivative is 2.5 Debye $\mathrm{Å^{-1}}$. All the intensities have the same scale, except for the first one, where the scale is multiplied by a factor 2

such observations will have to await the appearance of the next bright comet.

Acknowledgements. We gratefully acknowledge the support of the European Hale-Bopp Team members for the observations of comet Hale-Bopp. ALC and WDC thank the NASA Planetary Astronomy program for support.

References

Arpigny, C. 1976, in The Study of comets, IAU Coll., No. 25, NASA SP-393, 797
Baker, J., Bramble, S. K., & Hamilton, P. A. 1997, J. Mol. Spec., 183, 6
Becker, K. H., Tatarczyk, T., & Radić-Perić, J. 1979, Chem. Phys. Lett. 60, 3, 502
Chabalowski, C. F., Buenker, R. J., & Peyerimhoff, S. D. 1986, J. Chem. Phys., 84, 268
Clegg, R. E. S., & Lambert, D. L. 1982, MNRAS, 201, 723
Clementi, E., & Clementi, H. 1962, J. Chem. Phys., 36, 2824
Cochran, A. L., Cochran, W. D., & Barker, E. S. 2000, Icarus, 146, 583
Cooper, D. M., & Jones, J. J. 1979, J. Quant. Spectrosc. Radiat. Transfer, 22, 201
Denis-Gausset, L., & Sauval, A. J. 1968, Bull. Soc. Royale Sci. de Liège, 1-2, 48
Dossin, F., Ferhenbach, C., Haser, L., & Swings, P. 1961, Ann. d'Ap., 24, 519
Ferhenbach, C. 1963, C.R. (Paris), 256, 3788
Gausset, L., Herzberg, G., Algerqvist, A., Rosen, B. 1965, ApJ, 142, 45
Gredel, R., van Dishoeck, E. F., & Black, J. H. 1989, ApJ, 338, 1047
Herzberg, G. 1950, Molecular spectra and molecular structure I. Spectra of diatomic molecules (Van Nostrand Reinhold Company)
Herzberg, G. 1966, Molecular spectra and molecular structure III. Electronic spectra and electronic structure of polyatomic molecules (Van Nostrand Reinhold Company)
Hinkle, K. W., Keady, J. J., & Bernath, P. F. 1988, Science, 241, 1319
Jungen, C., & Merer, A. J. 1980, Mol. Phys., 40, 1, 95
Kurucz, L., Furenlid, I., Brault, J., & Testerman, L. 1984, National Solar Observatory Atlas Number, 1
Römelt, J., Peyerimhoff, S. D., & Buenker, J. 1978, Chem. Phys. Let., 58, 1, 1
Schmuttenmaer, C. A., Cohen, R. C., Pugliano, N., et al. 1990, Science, 249, 897
Stawikowski, A., & Greestein, J. L. 1964, ApJ, 140, 1280
Swings, P., Elvey, C. T., & Babcock, H. W. 1941, ApJ, 94, 320
Thekaekara, M. P. 1974, Appl. Opt., 13, 3, 518
Weltner, W. A., & Van Zee, R. J. 1989, Chem. Rev., 89, 1713
Zucconi, J. M., Festou, & M. C. 1985, A&A, 150, 180